A Model of the Gas Chromatographic Behavior of Polymer Stationary Phases through Their Glass Transitions

J.-M. Braun and J. E. Guillet*

Department of Chemistry, University of Toronto, Toronto, Canada M5S 1A1.

Received March 24, 1976

ABSTRACT: A computer model of the gas chromatographic behavior of polymer stationary phases is presented, based on the quantitative description of bulk and surface retention data in equilibrium conditions. At temperatures immediately above T_g where nonequilibrium chromatography prevails, it is assumed that penetration of solute molecules in the bulk of the polymer is incomplete and that the fractional volume of the polymer phase accessible to the solute increases with temperature at a rate proportional to the square root of D, the diffusion coefficient. It is shown that the effects on such computed retention diagrams of operating conditions, such as coating thickness and flow rate, and polymer properties, T_g and crystallinity, are satisfactorily accounted for.

Polymer stationary phases exhibit unusual retention characteristics in the vicinity of their glass transition temperature (T_g). Instead of the normal linear variation of the logarithm of the retention volume with absolute temperature, a z-shaped retention diagram is recorded. One such diagram, characterized by an increase in retention volume with temperature, is schematically represented in Figure 1. It has been shown[1] that at temperatures below T_g (region I), retention proceeded by surface adsorption. Owing to an increasing molecular mobility at and above T_g, penetration of solute molecules into the bulk of the polymer leads to reversal from the linear behavior (region II). At even higher temperatures (region III) equilibrium bulk retention occurs along with surface contributions.

There is ample experimental evidence[2–6] that the phenomenon first reported by Smidsrod and Guillet[1] for poly(N-isopropylacrylamide) is a general feature of all polymers undergoing their glass transitions. Reported failures[7–9] of the method to detect known transitions for some polymers have been satisfactorily accounted for by examining either the selected experimental conditions and/or the magnitude of polymer–solute interactions in the bulk and the surface of the stationary phase.[10,11] It has also been found[4,6] that the temperature of first deviation from linearity, T_1 in Figure 1, rather than the minimum of the retention diagram, should be identified with the glass transition temperature of the polymer as determined by thermal methods.

Nonequilibrium conditions in region II, characterized by a strong dependence of retention volumes on carrier gas flow rate, occur because of the slow diffusion of the solute molecules in the stationary polymer. Due to the rapid decrease of diffusion coefficient as the glass transition temperature is approached, equilibrium can no longer be established during the passage of the solute band through the column. As a result, the measured retention volumes depart from their equilibrium values (dashed line in Figure 1).

Because of the dual retention mechanism at temperatures above T_g, the shapes of the experimental retention diagrams are directly dependent on the surface to volume ratio of the stationary phase for an identical polymer–solute system. It has been shown[6] that the relation first suggested by Martin[12] to describe "liquid surface effects" on low molecular weight stationary phases is equally applicable to polymers for equilibrium retention volumes (region III),

$$V_R = K_b w_L + K_a A_L \tag{1}$$

where V_R is the retention volume, K_b and K_a the partition coefficients for bulk sorption and surface adsorption, w_L and A_L being the mass and surface area of the stationary phase. For thick polymer films (w_L/A_L large) a strong reversal from linear behavior is observed, while for very thin films nearly linear retention diagrams are recorded, corresponding almost exclusively to surface adsorption.[6]

In the present communication a computer model simulating the chromatographic behavior of polymer stationary phases through T_g is presented, based on the quantitative description of equilibrium retention volumes and including the effects leading to nonequilibrium conditions at temperatures immediately above T_g.

Results and Discussion

The existence of a single retention mechanism both below T_g for surface adsorption and under suitable conditions at temperatures above T_g for bulk sorption allows for a separate description of the corresponding surface and bulk retention volumes, V_{ads} and V_{bulk}. These read in their linear logarithmic form,

$$\ln V_{ads} = \ln A_L + \ln K_{a,0} - (\Delta H_a/RT) \tag{2}$$

and

$$\ln V_{bulk} = \ln w_L + \ln K_{b,0} - (\Delta H_s/RT) \tag{3}$$

where $-\Delta H_a$ and $-\Delta H_s$ are the heats of adsorption and solution determined from the slopes of the corresponding retention diagrams. In studies of polystyrene[6] and poly(acrylonitrile)[8] where surface adsorption was the only retention mechanism, no discontinuity in the temperature variation of the surface retention volume was detected at T_g. Thus eq 2 can be extrapolated to temperatures above T_g. As a result, retention volumes measured for concurrent retention mechanisms can be described by combination of eq 2 and 3, as expressed in eq 1.

To derive a mathematically tractable form for the bulk retention volume in the nonequilibrium region II it was assumed that the stationary phase could be divided into "active" and "inactive" fractions. In the "active" fraction the polymer–solute interaction would proceed under equilibrium conditions while in the "inactive" fraction the solute would not interact at all with the stationary phase. The active fraction, $X(T)$, could thus be pictured as corresponding to the extent of penetration of the solute molecules during the time of passage of the solute band. The bulk retention volume would thus be related, at any temperature T, to its equilibrium value by the relation,

$$V_{bulk} = X(T) K_b w_L \tag{4}$$

where $X(T)$ would be given by the ratio of the depth of penetration, $l(T)$, to the thickness of the stationary phase, L, with the limits $0 \leq X(T) \leq 1$. It can be shown that the average

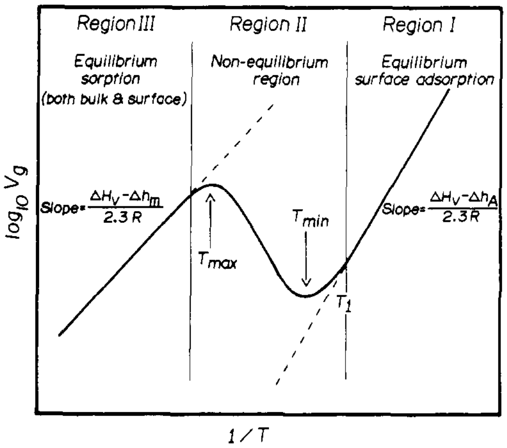

Figure 1. Typical retention diagram through T_g of polymer stationary phases.

distance traveled by the solute molecules in a slab of infinite thickness during time t is given by[13]

$$l(T) = \sqrt{2Dt} \tag{5}$$

where D is the diffusion coefficient. Due to the rapid decrease of the diffusion coefficient of small molecules in polymers as the temperature is lowered in the vicinity of T_g, equilibrium conditions can no longer be sustained during passage of the solute band through the column, giving rise to region II.

Considering that the solute molecules commonly used in GC are large organic molecules, the temperature variation of the diffusion coefficient in the vicinity of T_g should not, in general, be described by a simple Arrhenius relation. The formulation of Fujita et al.,[14] based on free volume theories, is more appropriate in this temperature range. At zero concentration of penetrant, one has,

$$\ln (D_0/RT) = \ln A_d - (B_d/f) \tag{6}$$

where D_0 is the equilibrium diffusion coefficient at infinite dilution, A_d and B_d are temperature-independent constants depending on the polymer–solute system, and f, the fractional free volume, is given by

$$f = f_g + \Delta\alpha(T - T_g) \tag{7}$$

where f_g is the fractional free volume at T_g, $\Delta\alpha$ the difference in thermal expansion coefficient above (α_l) and below (α_g) T_g. It is expected that, at infinite dilution of the probe, eq 6 should be directly applicable in GLC studies. Rather than computing diffusion coefficients for a particular polymer–solute system from literature values of the constants contained in eq 6 and 7, the flexibility of the model was preserved by evaluating the free volume parameters from the Simha–Boyer relation, known to be applicable to many polymers,[15,16]

$$\Delta\alpha T_g \simeq 0.11 \tag{8}$$

with f_g having its theoretical value of 0.025. B_d was set, as commonly done, equal to 1.[14]

The functional form of $l(T)$ can be derived from eq 5, i.e.,

$$l(T) \propto D^{1/2} \tag{9}$$

so that

$$l(T) \propto [RTA_d \exp(-1/f)]^{1/2} \tag{10}$$

Since A_d is a constant, depending only on the size of the solute molecule,[14] one can write

$$l(T) = [CT \exp(-1/f)]^{1/2} \tag{11}$$

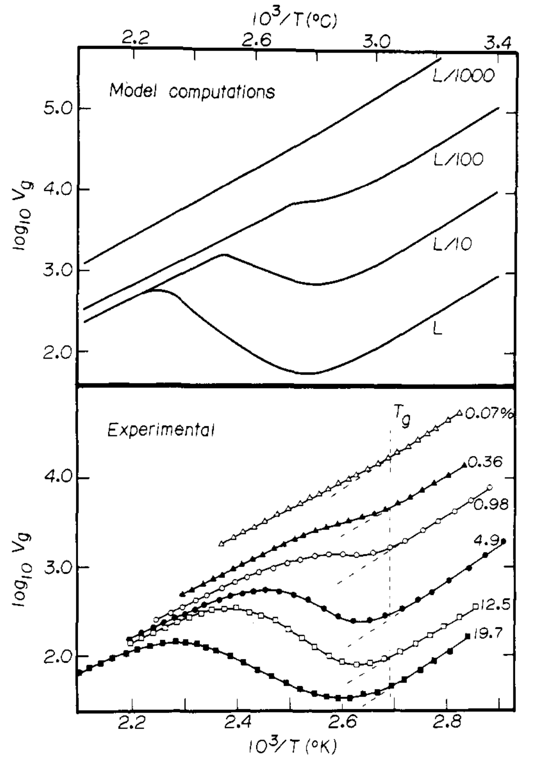

Figure 2. Computed retention diagrams, effect of coating thickness L, and experimental retention diagrams for n-hexadecane on polystyrene at various percent loadings.[6]

where the constant C can be fixed by considering that at temperatures high with respect to T_g equilibrium conditions prevail, i.e., $l(T)$ is large compared to L. Although setting an arbitrary value for this ratio determines the magnitude of the diffusion coefficient, this procedure does not affect the temperature variation of D as given by eq 6. Retention volumes can thus be calculated using a Fortran IV computer program over the whole temperature range encompassing T_g by summing, at each temperature, the relative contribution from surface adsorption and bulk sorption,

$$V_R = X(T)w_L K_{b,0} \exp(-\Delta H_s/RT) + A_L K_{a,0} \exp(-\Delta H_a/RT) \tag{12}$$

The numerical values for the partition coefficients K_a and K_b were taken, in the form of eq 2 and 3, from available experimental data on polystyrene with hydrocarbon probes.[10]

The effects of differing surface to volume ratios of the stationary phase on the retention diagrams were simulated by varying the thickness of the polymer film, L, at constant surface area A_L. The results of these changes, covering three orders of magnitude of "coating thickness", from L to $L/1000$, are shown in Figure 2 as computed retention diagrams. The features illustrated by these diagrams correspond quite closely to the experimental observations,[6] which are included in the bottom part of the figure for comparison. As L is decreased, the deviation from linear behavior becomes less pronounced, while the temperature of the maximum is shifted toward lower temperatures, extending the domain of equilibrium chromatography. The departure of bulk retention volumes from the common line recorded for the thinner stationary phases is clearly due to an ever-increasing contribution of surface adsorption to the overall retention.

Figure 3 shows a comparison of retention diagrams computed for identical average film thicknesses, but differing distributions, L and $L \pm \Delta L$. There is indeed little doubt that the coating thicknesses achieved on standard inert supports are far from uniform. In the case of a distribution of film

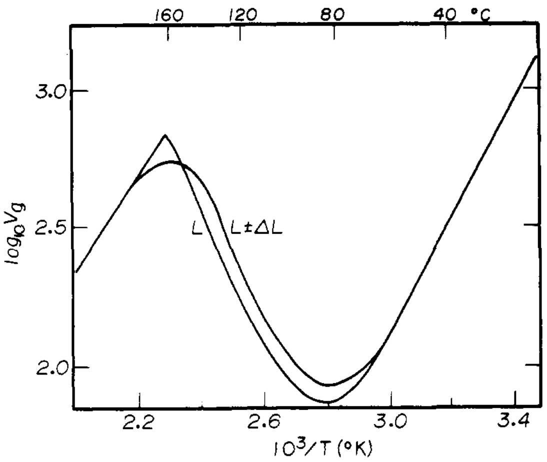

Figure 3. Computed retention diagrams: uniform film thickness, L, and distribution of thicknesses, $L \pm \Delta L$.

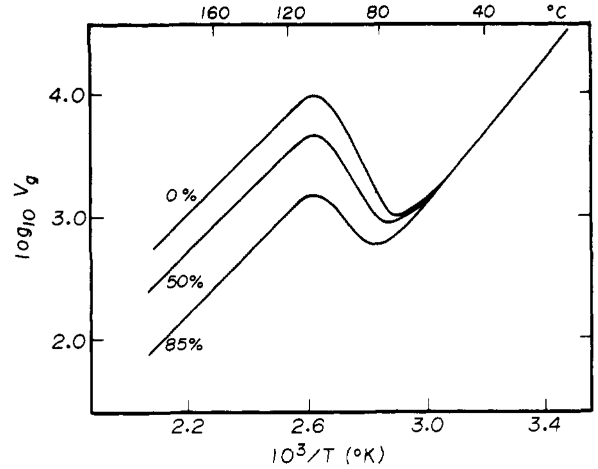

Figure 4. Computed retention diagrams: effect of crystallinity (%).

thicknesses, denoted $L \pm \Delta L$, as opposed to a uniform thickness of L, the computed retention diagram exhibits a more gradual departure from equilibrium bulk sorption, as evidenced by a round maximum. The thickness, centered around L, varied stepwise from $L/3$ to $3L$ ($L/3$ (10%), $L/\sqrt{3}$ (20%), L (40%), $L\sqrt{3}$ (20%), $3L$ (10%)). Other factors, such as a distribution of carrier gas velocities in the column, similarly contribute to a gradual departure from equilibrium conditions.

Up to the present point it has been implicitly assumed that the entire stationary phase could, at least in region III, interact with the solute molecules. It has been shown, however, that for crystalline polymers the bulk retention volume is proportional to the amorphous fraction only, thereby allowing for the determination of the crystalline content of polymer stationary phases from the relation[17]

$$V_{\text{bulk}} = (1 - X_c)K_b w_L \qquad (13)$$

where X_c is the crystalline weight fraction, $K_b w_L$ being obtained by extrapolation of the linear retention diagram recorded above the melting point (T_m) for the totally amorphous polymer. Upon substitution into eq 12 one then has for the retention volume of a semicrystalline polymer,

$$V_R = X(T)(1 - X_c)w_L K_{b,0} \exp(-\Delta H_s/RT) + A_L K_{a,0} \exp(-\Delta H_a/RT) \qquad (14)$$

In actual fact, whenever the melting curve is known, i.e., the variation of X_c with temperature, eq 14 represents the variation of the retention volume through both T_g and T_m. The effects of crystalline content on computed retention diagrams are shown in Figure 4 for three crystallinities, 0, 50, and 85% at identical film thickness. It was assumed in these computations that neither the solubility of the solute in the amorphous domains nor the diffusion coefficient were affected by crystalline content. It is seen that as the crystallinity of the stationary phase increases, reversal from the linear behavior, and hence detection of the transition, becomes less pronounced, akin to a decrease in film thickness. It is believed that in some cases failure to detect the glass transition of highly crystalline materials, as reported for isotactic polypropylene,[9] is due to such phenomena.

It should be pointed out that eq 14 can be given a broader, though qualitative interpretation. It is indeed immaterial whether a decrease in bulk retention volume is brought about by an increase in crystallinity or by a decrease in solubility of the probe in the bulk polymer. One could thus regard X_c of eq 14 as an adjustable parameter describing either the effects of crystallinity or probe solubility. It has been found that despite favorable operating conditions (very thick films) detection of T_g was impossible or nearly so for alkanes on poly(acrylonitrile)[8] and perfluoroalkanes on polystyrene[10] due to an extremely low solubility of the probe molecule in the polymer.

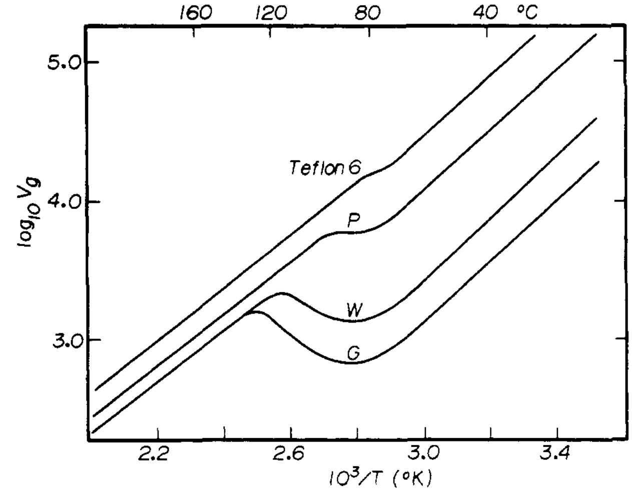

Figure 5. Computed retention diagrams: effect of surface area of inert support.

In contrast to standard GLC, the type of support chosen is quite important when investigating polymers near T_g. The equivalence of inert supports reported in the literature pertains to the variation in density of these materials and expresses the required loadings to achieve certain separations. Reversal from the linear behavior recorded with polymers depends on the weight, but also on the surface area of the stationary phase. This is illustrated in Figure 5 showing the variation in computed retention diagrams calculated using the reported surface areas of common inert supports, Chromosorb P, W, and G, and Teflon 6, at identical weight loading of polymer. Owing to the differing densities and surface areas[18] of these supports, the resultant retention diagrams are quite different. In particular, it is worth noting that significantly higher loadings are required on Teflon 6 and Chromosorb P to achieve invariance of bulk retention volumes owing to the higher surface area of these supports. In this respect it should be noted that the coverage ratio (gram polymer/gram support) commonly used to gauge the likelihood of surface adsorption in GLC is of little help when comparing different supports. In the present case, variation of the surface to volume ratio by as much as a factor of 20 would occur at identical coverage ratio for different supports.

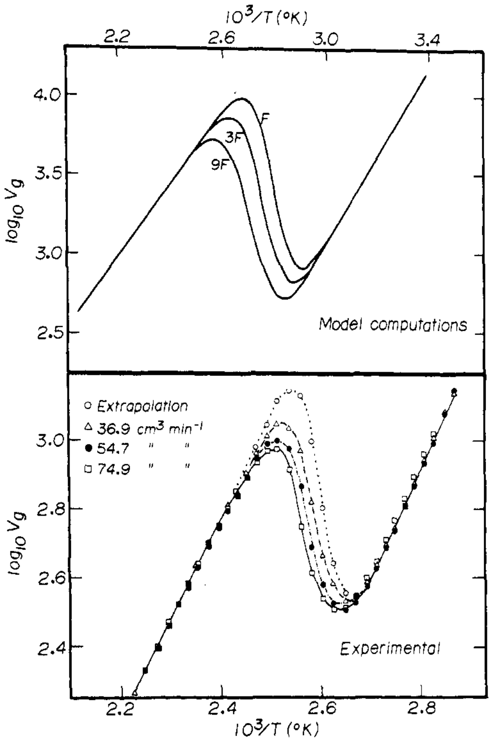

Figure 6. Computed retention diagrams at various flow rates F, and experimental retention diagrams for n-hexadecane on polystyrene.[6]

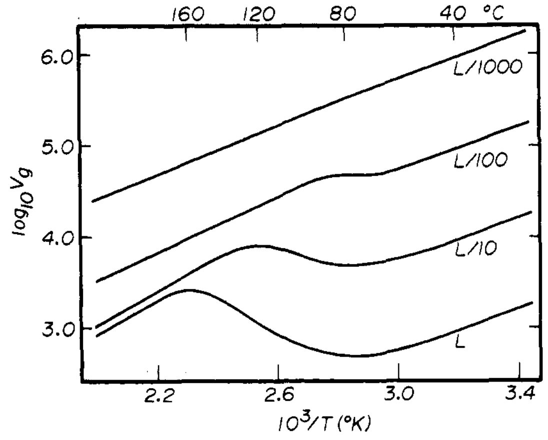

Figure 7. Computed retention diagrams: effect of coating thickness, L, for $-\Delta H_a < -\Delta H_s$.

As stated in eq 5 the depth of penetration is proportional to both the diffusion coefficient and time, and one should write

$$l(T,t) = [CT\exp(-1/f)]^{1/2}(t)^{1/2} \tag{15}$$

In gas chromatography such time-dependent effects show up as flow-rate-dependent retention volumes since

$$t_R = V_R/F \tag{16}$$

where t_R is the retention time and F the flow rate. If one includes the proportionality factor between t and t_R in constant C, t_R (or F) appears in eq 15 and one now has for the retention volume,

$$V_R = X(T,t)(1 - X_c)w_L K_{b,0}\exp(-\Delta H_s/RT) + A_L K_{a,0}\exp(-\Delta H_a/RT) \tag{17}$$

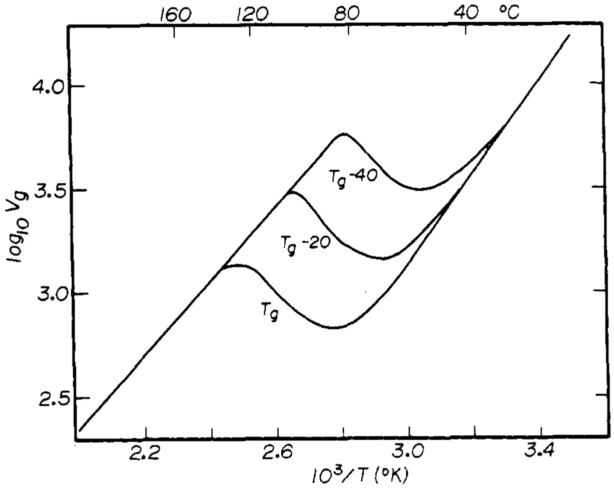

Figure 8. Computed retention diagrams: effect of T_g.

Figure 6 represents the computed retention diagrams obtained at three different flow rates, covering a nearly tenfold change in flow rate. As recorded experimentally,[6] a drastic dependence of retention volumes is detected in region II while the temperature of the maximum is shifted toward higher temperatures as the flow rate is increased. The observed increase in retention volume with decreasing flow rate is expected since, as expressed in eq 15, the polymer–solute system is allowed to come closer to equilibrium.

While the present model adequately describes the various column parameters and operating conditions, it can also be useful in comparing different polymer–solute systems. It has been noted that, in general, the heat of adsorption, $-\Delta H_a$, is systematically larger than the corresponding heat of solution, $-\Delta H_s$, for any one polymer–solute system.[10] If such were not the case, quite unusual retention diagrams would be recorded with polymers near T_g. This is illustrated in Figure 7 depicting the effects of coating thickness, L, for a polymer–solute system characterized by a larger (arbitrarily chosen) heat of solution as compared to its heat of adsorption. It is seen that, although the detection of T_g remains unaffected, several changes in the retention diagram take place. Due to the larger rate of decrease of the bulk retention volume with increasing temperature, surface adsorption becomes again the predominant retention mechanism at high temperatures (region III) for the smaller film thicknesses as evidenced by a change in slope. Even for the thickest film (L) it is not immediately apparent whether true bulk retention volumes can be measured without extrapolation of retention volumes to infinite thickness of the stationary phase. No such uncommon retention behavior has yet been reported.

Figure 8 shows the effects on computed retention diagrams of the location of the glass transition temperature in otherwise identical conditions of polymer–solute interaction and film thickness. It had indeed been observed[4] that for both poly(methyl methacrylate) of various tacticities and plasticized poly(vinyl chloride)'s the region of equilibrium bulk sorption extended toward lower temperatures as tacticity or degree of plasticization was changed. As is clearly apparent from eq 6 and 7 a decrease in the glass transition temperature brings about an increase in diffusion coefficient, at identical temperature, thereby allowing equilibrium conditions to be sustained at increasingly lower temperatures.

The extent of nonequilibrium (region II), while dependent on experimental conditions, is drastically affected by polymer properties. A case in point is poly(isobutylene) for which the nonequilibrium region has been shown to span a considerable range of temperature, from about −70 (T_g) to +50 °C.[19] Despite a dearth of GLC data at very low temperatures, there is evidence that equilibrium bulk sorption is achieved below

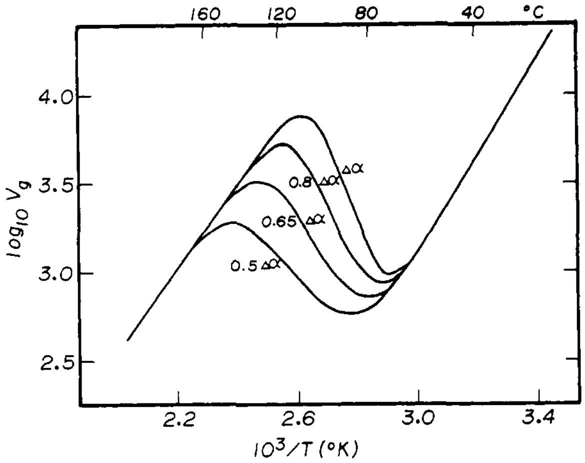

Figure 9. Computed retention diagrams: effect of expansion coefficient, $\Delta\alpha = \alpha_l - \alpha_g$.

room temperature for natural rubber stationary phases[20] ($T_g \simeq -70$ °C) and a styrene–butadiene copolymer ($T_g \simeq -60$ °C).[4] Such widely differing chromatographic behavior can, however, be understood. As shown by Chen and Ferry[21] in an investigation of polydienes and poly(isobutylene), both fractional free volumes and diffusion coefficients can be significantly different for polymers characterized by nearly identical glass transition temperatures. In particular, the diffusion coefficient at 25 °C for hexadecane in natural rubber was larger by about two orders of magnitude than in poly(isobutylene), accounting quite clearly for the chromatographic observations. If in the present model one then allows the temperature variation of the diffusion coefficient to depart from the values computed from eq 6 and 7, e.g., by changing the thermal expansion coefficient $\Delta\alpha$, similar differences in computed retention diagrams are recorded, as shown in Figure 9. Due to a decrease in $\Delta\alpha$, hence in f and D, higher temperatures are required to achieve equilibrium conditions, as evidenced by an increase in the temperature of the maximum of the retention diagram. Quite clearly, if the chromatographic behavior of one particular polymer–solute system is to be investigated, the exact variation of D with temperature must be known.

It should also be noted that the temperature variation of the diffusion coefficient assumed in the present work, Fujita's free volume derivation, is not a prerequisite for observing a z-shaped retention diagram. While eq 6 differs markedly from an Arrhenius temperature variation for D in the immediate vicinity of T_g, both formulations become similar at higher temperatures ($T > T_g + 50$). As is clearly apparent from Figure 2, nonequilibrium and a maximum in the retention diagram can be obtained, for thick stationary phases, at high temperatures where an Arrhenius variation of the diffusion coefficient would be expected.

Conclusions

A very satisfactory agreement is obtained between experimentally determined retention diagrams and those computed with the present model. By including a description of the nonequilibrium region based on free volume theories for the temperature variation of the diffusion coefficient to the treatment of simultaneous occurrence of surface adsorption and bulk sorption, the salient features of the chromatographic behavior of polymers near T_g are suitably reproduced. The present model allows for the possibility of either introducing known retention data and free volume parameters or using it as a purely predictive tool. The uncharacteristic chromatographic behavior of poly(isobutylene) is discussd in those terms and accounted for in the light of the polymer's frictional properties.

Acknowledgment. The authors wish to acknowledge the financial support of the National Research Council of Canada and the Dunlop Research Centre of Sheridan Park, Ontario, and a scholarship from the Canada Council (to J.-M. Braun).

References and Notes

(1) O. Smidsrod and J. E. Guillet, *Macromolecules*, **2**, 272 (1969).
(2) A. Lavoie and J. E. Guillet, *Macromolecules*, **2**, 443 (1969).
(3) J. R. Wallace, P. J. Kozak, and F. Noel, *SPE J.*, 43 (1970).
(4) J.-M. Braun, A. Lavoie, and J. E. Guillet, *Macromolecules*, **8**, 311 (1975).
(5) N. Valentin, B. Chabert, J. Chauchard, and G. Edel, *Bull. Sci. ITF*, **3**, 5 (1974).
(6) J.-M. Braun and J. E. Guillet, *Macromolecules*, **8**, 882 (1975).
(7) S. A. Liebman, D. H. Ahlstrom, and C. R. Foltz, *J. Chromatogr.*, **67**, 153 (1972).
(8) J. E. Guillet and M. Galin, *J. Polym. Sci., Polym. Lett. Ed.*, **11**, 223 (1973).
(9) S. Galassi and G. Audisio, *Makromol. Chem.*, **175**, 2975 (1974).
(10) J.-M. Braun, Ph.D. Dissertation, University of Toronto, 1975.
(11) J.-M. Braun and J. E. Guillet, *Macromolecules*, **9**, 340 (1976).
(12) R. L. Martin, *Anal. Chem.*, **33**, 347 (1961).
(13) W. J. Moore, "Physical Chemistry", Prentice Hall, Englewood Cliffs, N.J., 1962.
(14) H. Fujita, A. Kishimoto, and K. Matsumoto, *Trans. Faraday Soc.*, **56**, 424 (1960).
(15) R. Simha and R. F. Boyer, *J. Chem. Phys.*, **37**, 1003 (1962).
(16) R. F. Boyer and R. Simha, *J. Polym. Sci., Polym. Lett. Ed.*, **11**, 33 (1973).
(17) J. E. Guillet and A. N. Stein, *Macromolecules*, **3**, 102 (1970).
(18) D. M. Ottenstein, *J. Chromatogr. Sci.*, **11**, 136 (1973).
(19) J.-M. Braun and J. E. Guillet, *Macromolecules*, **8**, 557 (1975).
(20) Y. B. Tewari and H. P. Schreiber, *Macromolecules*, **5**, 329 (1972).
(21) S. P. Chen and J. D. Ferry, *Macromolecules*, **1**, 270 (1968).